Target Dependence of Angular Distributions for Near-Threshold (e,2e) Processes

Cheng Pan and Anthony F. Starace

Department of Physics and Astronomy, The University of Nebraska, Lincoln, Nebraska 68588-0111

(Received 13 March 1991)

Distorted-wave calculations of the triply differential cross sections for electron-impact ionization of H and He targets are presented for final-state electrons sharing 4-eV excess energy and leaving in opposite directions. The experimentally observed target dependence of the angular distributions is shown to stem essentially from short-range effects on the s-wave phase shifts of both incident and final-state continuum electrons.

PACS numbers: 34.80.Dp

Electron-impact-ionization processes are of theoretical importance as a means of understanding the fundamental problem of three or more particles interacting via Coulomb forces. For final states having two free electrons, i.e., (e,2e) processes, the prediction of triply differential cross sections provides a most severe test of theoretical understanding [1,2]. Recent low-energy (e,2e) experiments [3–5] for various targets have shown the triply differential cross sections to be highly dependent on the target even though at asymptotic separations the long-range fields in the final state are target independent. While the form of the triply differential cross section is known [6], numerical calculations are required to deduce the effect of a particular target on the (e,2e) process. However, even higher-order or distorted-wave theoretical calculations [7–9], some of which [8] incorporate the proper asymptotic boundary conditions [10], have been carried out only for electron-impact energies well above threshold. While the Wannier theory [11–14] for the threshold energy dependence has been analyzed for all contributing partial waves [15–17], numerical estimates of their relative importance, which are essential for describing the triply differential cross sections, have not heretofore been made. We report here theoretical calculations of triply differential cross sections for electron-impact ionization of H and of He which do estimate the magnitude of each partial-wave contribution and provide an explanation of the origin of the target effects recently observed experimentally [3,4].

The key features of our theoretical approach may be stated simply. We employ distorted waves to describe both initial and final states. We also restrict our consideration to final states for which the two electrons share 4 eV of kinetic energy and in which the angle between their momenta, θ_{12}, is π. Experimental data are available [3,4] on the triply differential cross sections for such final states as a function of the angle θ_1 which one of the final-state electrons makes with the incident electron beam. We approximate the final-state electron-electron interaction by a variationally determined screening potential [18–20]. In what follows we expand upon our theoretical approach, compare our predictions with available experimental measurements, and discuss the origins of the target effects observed experimentally.

For infinite nuclear mass, the differential cross section for electron-impact ionization [8(a)] becomes (in a.u.)

$$\frac{d\sigma}{d\mathbf{k}_1 d\mathbf{k}_2} = \frac{(2\pi)^4}{k} |\langle \Psi_f^- | V | \Phi_i^+ \rangle|^2 \delta(E_f - E_i). \quad (1)$$

In Eq. (1), k is the magnitude of the momentum of the incident electron, $\mathbf{k}_1$ and $\mathbf{k}_2$ are the momenta of the two continuum electrons in the final state, and E_i and E_f are the energies of the initial and final states. The perturbation V is the difference between the exact Hamiltonian and the approximate Hamiltonian used to construct Φ_i^+, the distorted wave used to describe approximately the initial state. In our calculations V is defined by

$$V \equiv \sum_{i=1}^{N} \frac{1}{|\mathbf{r}_{N+1} - \mathbf{r}_i|} - V_{HF}^{N+1}(\mathbf{r}_{N+1}), \quad (2)$$

where the first term on the right-hand side of Eq. (2) is the Coulomb interaction between the incident electron and the N target electrons and the second term is a Hartree-Fock (HF) approximation to this interaction which we use in constructing Φ_i^+. (More specifically, the radial wave functions describing the incident electron for each partial-wave contribution to Φ_i^+ are calculated in the appropriate term-dependent HF potential.) Omitted in Eq. (2) are corrections to our description of the target by hydrogenic wave functions in the case of H and by ground-state HF wave functions in the case of He. Such corrections stem from interactions between the incident electron and the target electrons (e.g., polarization effects) as well as, in the case of He, electron correlations among the target electrons themselves. We emphasize that our inclusion of V_{HF}^{N+1} in the description of the initial state is an improvement upon the typical description of the incident electron by a plane wave. In particular, it is needed to describe theoretically the experimentally observed target effects.

The final-state wave function Ψ_f^- in Eq. (1) should be, in principle, the exact solution to the full Hamiltonian satisfying the exact boundary conditions [10] for two continuum electrons moving in the Coulomb field of the ionized target. We have expanded our final-state wave function in independent-electron states for the two continuum electrons and have coupled their orbital and spin angular momenta to partial waves characterized by L and S. For H, L and S are the total orbital and spin angular momenta of the system and are thus eigenstates of the collision.

For He, S must be coupled to the spin of the target electron to form the system's spin, which equals $\frac{1}{2}$. Thus, in He, the target electron couples singlet and triplet states of the continuum-electron pair. However, we have ignored such interchannel coupling in the case of He and treat the channels designated by L and S as uncoupled.

The major approximation to Ψ_f^- in our calculations is our replacement of the exact Coulomb interaction between the two continuum electrons by a variationally determined screening potential [18–20]. For the configuration considered here in which $\hat{k}_1 = -\hat{k}_2$, the effective charges Δ_1 and Δ_2 are determined by the condition [18–20]

$$-\frac{Z_T-\Delta_1}{k_1} - \frac{Z_T-\Delta_2}{k_2} = -\frac{Z_T}{k_1} - \frac{Z_T}{k_2} + \frac{1}{k_1+k_2}, \qquad (3)$$

where Z_T is the net asymptotic charge of the ionized target. In our calculations we satisfy Eq. (3) using the following screening charges [20]:

$$\Delta_i \equiv \frac{k_i^2}{(k_1+k_2)^2} \quad (i=1,2). \qquad (4)$$

The exact Coulomb interaction in our calculations is replaced by the sum of the following screening potentials $(i=1,2)$:

$$V_i(k_1,k_2) = \Delta_i y_0(r), \qquad (5)$$

where $y_0(r)$ is chosen to have the properties $y_0 \to 0$ as $r \to 0$ and $y_0 \to 1/r$ as $r \to \infty$.

The screening potentials V_1 and V_2 in Eq. (5) are included in the equations we use to calculate the radial wave functions for the two final-state continuum electrons for each pair of orbital angular momenta (l_1,l_2) and each partial wave LS, where $l_1 \oplus l_2 = L$, and $\frac{1}{2} \oplus \frac{1}{2} = S$. In H, each of the continuum electrons sees only the Coulomb field of the proton and the appropriate screening potential V_i. In He, each of the continuum electrons experiences an LS-dependent HF-type interaction with the residual He$^+$ ion plus the appropriate screening potential V_i. For the asymptotic final-state configuration considered here in which $\hat{r}_1 = \hat{k}_1$, $\hat{r}_2 = \hat{k}_2$, and $r_1/r_2 = k_1/k_2$ the screening potentials V_i in Eq. (5) introduce a phase which differs

FIG. 1. Relative triply differential cross sections [cf. Eq. (7)] for $\theta_{12}=\pi$ and $\frac{1}{2}k_1^2 = \frac{1}{2}k_2^2 = 2$ eV for (a) H and (b) He targets. Solid (dashed) curves: Present results including (not including) the effective screening potential [cf. Eq. (5)]. Open circles: Experimental results of Schlemmer *et al.* [4]. Solid triangles: Experimental results of Selles, Huetz, and Mazeau [3].

from the correct asymptotic phase [10] only by terms which are independent of r_1 and r_2.

Using the initial- and final-state wave functions described above in Eq. (1), summing over all final-state magnetic quantum numbers, averaging over all initial-state magnetic quantum numbers, and integrating over the kinetic energy of one of the final-state continuum electrons [in order to remove the δ function in Eq. (1)], one obtains the following expression for the triply differential cross section [21]:

$$\frac{d^3\sigma}{dE_1 d\Omega_1 d\Omega_2} = \frac{\pi}{4k^2} \sum_{LL'} \sum_S A(LS)A^*(L'S) \sum_\lambda P_\lambda(\hat{k}_1 \cdot \hat{k}) [L][L'][\lambda] \begin{bmatrix} L & L' & \lambda \\ 0 & 0 & 0 \end{bmatrix}^2. \qquad (6)$$

In Eq. (6), the symbol $[x] \equiv 2x+1$, $E_1 = k_1^2/2$, $d\Omega_i$ is the solid angle element for the momentum k_i, L and S are the orbital and spin angular momenta of the coupled pair of final-state continuum electrons, P_λ is a Legendre polynominal, and $A(LS)$ is the dynamical scattering amplitude for the LS partial wave.

Further details of the derivation of Eq. (6), in particular details concerning the calculation of the amplitudes $A(LS)$, will be presented elsewhere [21]. We note, however, that since $\theta_{12}=\pi$, $A(LS)$ is nonzero only when the parity of the final-state continuum-electron pair equals
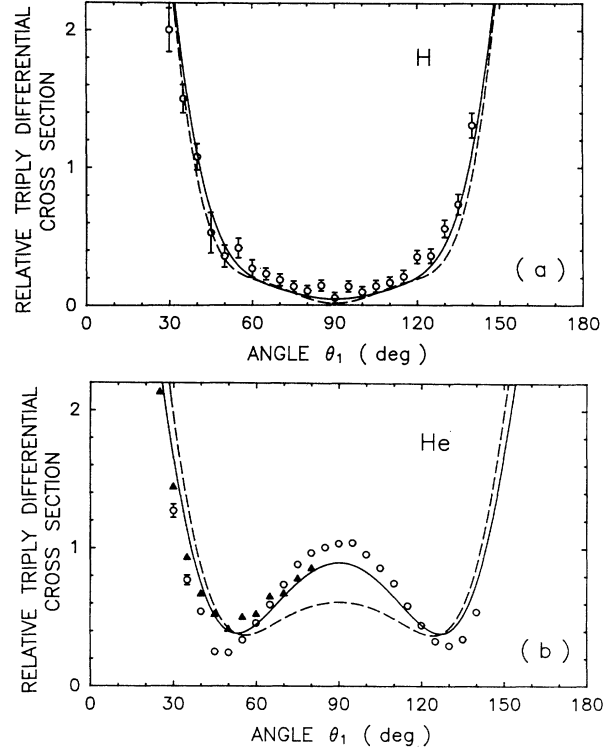
$(-1)^L$. In addition, for the equal-energy-sharing case, in which $k_1=k_2$, $A(LS)$ is nonzero only when the parity of the final-state electron pair equals $(-1)^S$. Hence, for the equal-energy-sharing case, only the $^1S^e$, $^3P^o$, $^1D^e$, $^3F^o$, ... partial waves LS of the final-state electron pair contribute [16,17]. Since in Eq. (6) each of the amplitudes in the product $A(LS)A^*(L'S)$ must have the same spin S, and since the $3j$ symbol is nonzero only if $(-1)^{L+L'+\lambda}$ is even, we conclude that for the case of $k_1=k_2$ only even values of λ contribute. Thus the angu-

lar distribution is symmetric about $\theta_1 = \pi/2$. When $k_1 \neq k_2$, the $^3S^e$, $^1P^o$, $^3D^e$, $^1F^o$,... partial waves may also contribute and hence terms with odd values of λ occur, leading to a loss of symmetry about $\theta_1 = \pi/2$.

Our results for the equal-energy-sharing case, $\frac{1}{2} k_1^2 = \frac{1}{2} k_2^2 = 2$ eV, are shown in Fig. 1 for both H and He targets. Since the experimental data are relative, we plot the relative triply differential cross sections

$$\frac{4\pi}{\sigma} \frac{d^3\sigma}{dE_1 d\Omega_1 d\Omega_2} \equiv 1 + \sum_{\lambda > 0} \beta_\lambda P_\lambda(\hat{\mathbf{k}}_1 \cdot \hat{\mathbf{k}}) , \qquad (7)$$

where σ and β_λ are defined by comparison of Eq. (7) with Eq. (6). The relative experimental data were fitted by our results using Eq. (7) and a standard least-squares procedure.

In agreement with the experimental data shown, our triply differential cross section for H has a minimum at $\theta_1 = \pi/2$ while that for He has a local maximum at this angle. Two theoretical results are shown for each target: those with and those without inclusion of the final-state electron-electron screening potential defined in Eq. (5). While inclusion of this screening potential has a negligible effect on the calculations for H, in the case of He it improves agreement with experiment significantly.

The key features of the triply differential cross sections for H and for He may be understood from examination of our calculated amplitudes in Table I. In this table we have given the relative magnitudes and phases of the amplitudes for the first six partial waves LS of the final-state pair of continuum-energy electrons. While the absolute magnitudes of these amplitudes are quite different for H and for He, the relative magnitudes of these amplitudes, which determine the angular distribution, are quite similar. As was found empirically [4], the partial waves for $L > 3$ are not important: In our calculations they are an order of magnitude smaller than those for $L \leq 3$. Note also that the triplet amplitudes for $L = 1$ and 3 are comparable in magnitude to the singlet amplitudes for $L = 0$ and 2. They thus cannot be neglected, as was done in a recent calculation for helium [22].

The major difference between H and He in our calculations is between the arguments of the ^1S partial-wave amplitudes, which differ by more than 1.6 rad. This difference affects the triply differential cross sections in Eq. (6) primarily via the interference terms between the $L=0$ and 2 partial waves which contribute to the coefficient of the $\lambda = 2$ Legendre polynominal. These interference terms in H and in He have phases which differ by more than 1.3 rad. We have tested whether the sum $A(^1S^e)A^*(^1D^e) + A(^1D^e)A^*(^1S^e)$ is responsible for the different observed angular distributions in H and in He by artificially replacing the s-wave partial-wave phase shifts of the incident electron as well the two final-state continuum electrons in the calculation of the $A(^1S^e)$ amplitude for He by the corresponding calculated s-wave phase shifts used in our H calculation. This numerical experiment results in the calculated He triply differential cross section having an angular distribution similar to that for H. These independent-electron s-wave phase shifts are affected most by the short-range interactions which produce the target dependence observed experimentally [4].

In Fig. 2 we present our relative triply differential cross-section results for the unequal-energy-sharing case,
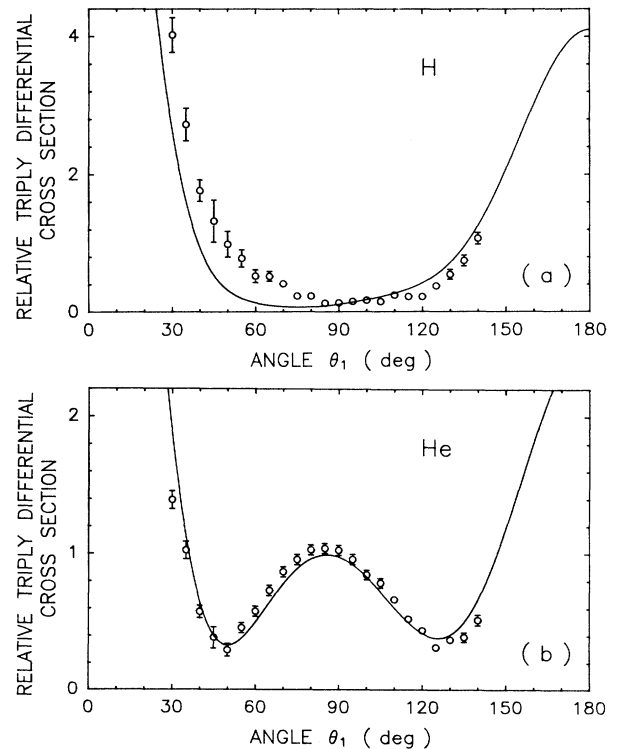

FIG. 2. Relative triply differential cross sections [cf. Eq. (7)] for $\theta_{12} = \pi$, $\frac{1}{2} k_1^2 = 3.5$ eV, and $\frac{1}{2} k_2^2 = 0.5$ eV for (a) H and (b) He targets. Solid curves: Present results including the effective electron-electron screening potential [cf. Eq. (5)]. Open circles: Experimental results of Schlemmer et al. [4].

TABLE I. Relative amplitude and phase for the electron-impact ionization scattering amplitudes $A(LS)$ for H and for He targets for final-state electron kinetic energies $\frac{1}{2} k_1^2 = \frac{1}{2} k_2^2 = 2$ eV.

Partial wave $^{2S+1}L^\pi$	Relative amplitude $|A(LS)|/|A(^1S^e)|$		arg $A(LS)$ (rad)	
	H	He	H	He
$^1S^e$	1.0000 [a]	1.0000 [a]	4.447	6.067
$^3P^o$	0.4342	0.4275	2.711	2.947
$^1D^e$	0.4760	0.5276	3.992	4.267
$^3F^o$	0.3259	0.2183	3.090	3.017
$^1G^e$	0.0463	0.0376	3.217	3.220
$^3H^o$	0.0345	0.0150	2.793	2.482

[a]For H, $|A(^1S^e)| = 0.3229$; for He, $|A(^1S^e)| = 0.2193$.

$\frac{1}{2}k_1^2 = 3.5$ eV and $\frac{1}{2}k_2^2 = 0.5$ eV, for both H and He targets. The experimental data [4] shown were once again fitted by our results using a least-squares procedure. The shapes of the angular distributions are very similar to those in Fig. 1, except now there is no symmetry about $\theta_1 = \pi/2$. The triply differential cross sections are largest for $\theta_1 \approx 0$, i.e., when the higher-energy electron is ejected in the direction of the incident beam. For the case of H, our calculations show a minimum in the neighborhood of 75° while the experimental results show a minimum close to 90°. Otherwise, agreement between theory and experiment is quite reasonable. For the case of He, agreement of theory and experiment is excellent. A detailed discussion of the scattering amplitudes $A(LS)$ for the unequal-energy-sharing case will be presented elsewhere [21]. Suffice it to say here that for the partial waves having even values of $L + S$, the magnitudes and phases are similar to those given in Table I for the equal-energy case. In contrast, for the partial waves having odd values of $L + S$, the magnitudes for $L \leq 3$ are much smaller than those for the same L having even values of $L + S$, while for $L > 3$, the reverse is generally true.

In conclusion, we have presented distorted-wave calculations of the triply differential cross sections for electron-impact ionization of H and He targets for the final-state configuration in which $\theta_{12} = \pi$ and the continuum-electron pair share 4-eV excess final-state energy. Our results represent the first theoretical analysis of the target effects observed experimentally in the near-threshold energy region [3–5]. These effects have been shown to stem primarily from differences in the interference of $^1S^e$ and $^1D^e$ partial-wave amplitudes of the final-state electron pair for the H and He targets. These differences in turn stem largely from short-range effects on the s-wave phase shifts of both the incident and the final-state continuum electrons in the two cases. A more detailed presentation of the present results for H and He targets as well as a similar analysis for Ne, Ar, and Kr targets will be presented elsewhere [21].

Note added.— After submitting this paper, we learned that Brauner *et al.* [23] have extended their calculations for $(e, 2e)$ processes in H to the threshold energy region. For $\theta_{12} = \pi$, their angular distribution results and ours agree, as discussed elsewhere [21].

[1] *Electron Impact Ionization,* edited by T. D. Märk and G. H. Dunn (Springer, New York, 1985).
[2] H. Ehrhardt, K. Jung, G. Knoth, and P. Schlemmer, Z. Phys. D **1**, 3 (1986).
[3] P. Selles, A. Huetz, and J. Mazeau, J. Phys. B **20**, 5195 (1987).
[4] P. Schlemmer, T. Rösel, K. Jung, and H. Ehrhardt, Phys. Rev. Lett. **63**, 252 (1989).
[5] P. Selles, J. Mazeau, and A. Huetz, J. Phys. B **23**, 2613 (1990).
[6] P. L. Altick, J. Phys. B **18**, 1841 (1985).
[7] F. Mota Furtado and P. F. O'Mahony, J. Phys. B **22**, 3925 (1989).
[8] (a) M. Brauner, J. S. Briggs, and H. Klar, J. Phys. B **22**, 2265 (1989); (b) M. Brauner, J. S. Briggs, and J. T. Broad, J. Phys. B **24**, 287 (1991).
[9] X. Zhang, C. T. Whelan, and H. R. J. Walters, J. Phys. B **23**, L173 (1990); E. P. Curran, C. T. Whelan, and H. R. J. Walters, J. Phys. B **24**, L19 (1991).
[10] P. J. Redmond (unpublished); see L. Rosenberg, Phys. Rev. D **8**, 1833 (1973), and Ref. [8].
[11] G. H. Wannier, Phys. Rev. **90**, 817 (1953).
[12] A. R. P. Rau, Phys. Rev. A **4**, 207 (1971); Phys. Rep. **110**, 369 (1984).
[13] R. Peterkop, J. Phys. B **4**, 513 (1971); **16**, L587 (1983).
[14] See also J. M. Feagin, J. Phys. B **17**, 2433 (1984), and references therein.
[15] H. Klar and W. Schlecht, J. Phys. B **9**, 1699 (1976).
[16] C. H. Greene and A. R. P. Rau, Phys. Rev. Lett. **48**, 533 (1982); J. Phys. B **16**, 99 (1983).
[17] A. D. Stauffer, Phys. Lett. **91A**, 114 (1982).
[18] M. R. H. Rudge and M. J. Seaton, Proc. Roy. Soc. London A **283**, 262 (1965).
[19] R. K. Peterkop, *Theory of Ionization of Atoms by Electron Impact* (Colorado Associated Univ. Press, Boulder, CO, 1977), pp. 128 and 129.
[20] S. Jetzke, J. Zaremba, and F. H. M. Faisal, Z. Phys. D **11**, 63 (1989); F. H. M. Faisal, in *Atoms in Strong Fields,* edited by C. A. Nicolaides, C. W. Clark, and M. H. Nayfeh (Plenum, New York, 1990), pp. 407–424.
[21] C. Pan and A. F. Starace (to be published).
[22] D. S. F. Crothers, J. Phys. B **19**, 463 (1986).
[23] M. Brauner, J. S. Briggs, H. Klar, J. T. Broad, T. Rösel, K. Jung, and H. Ehrhardt, J. Phys. B **24**, 657 (1991).